Available online at www.sciencedirect.com

ScienceDirect

Procedia CIRP 85 (2019) 299–304

www.elsevier.com/locate/procedia

2nd CIRP Conference on Composite Material Parts Manufacturing (CIRP-CCMPM 2019)

Chip formation in machining of unidirectional carbon fibre reinforced polymer laminates: FEM based assessment

F. Cepero-Mejias[a,b,c,*], J.L. Curiel-Sosa[b,c], K. Kerrigan[d], V.A. Phadnis[d]

[a] *Industrial Doctorate Centre in Machining Science, The University of Sheffield, Sir Frederick Mappin Building, Mappin Street, S1 3JD Sheffield, United Kingdom.*
[b] *Computer-Aided Aerospace & Mechanical Engineering (CA2M) Research Group, Sir Frederick Mappin Building, Mappin Street, S1 3JD Sheffield, United Kingdom.*
[c] *Department of Mechanical Engineering, The University of Sheffield, Sir Frederick Mappin Building, Mappin Street, S1 3JD Sheffield, United Kingdom.*
[d] *AMRC with Boeing, Advanced Manufacturing Park, Wallis Way, Catcliff, Rotherham, S605TZ, United Kingdom.*

Abstract

Finite-element (FE) method offers a low cost virtual alternative to assist in optimisation of critical process parameters in machining of composites. This study is focussed on understanding the mechanics of chip formation in orthogonal cutting of unidirectional (UD) carbon-fibre-reinforced polymer (CFRP) laminates through development of FE models. Machining responses of UD CRFP laminates with fibre orientation of 45° (measured with respect to the cutting direction) are assessed. Modelling of material removal in the form of fragmented chips is considered. Damage initiation is determined using the Hashin stress criterion for the fibre component, while matrix failure predicted using Puck criteria. Subsequent damage evolution events are modelled using a strain-based softening approach to degrade relevant material properties linearly. Primary numerical results compared with experimental data revealed that developed FE models are able to predict global machining responses (i.e. cutting forces) and characterise various discrete damage modes associated with machining response of quasi-brittle CFRP laminates successfully. The models also provide a valuable insight into variation in chip morphology.

Keywords: Machinnig; Composite; Damage; Hashin failure criteria; Orthogonal cutting; Puck failure criterion; Finite element

1. Introduction

In the last decades, the use of polymer matrix composites (PMCs) have experience a steady increase in high-tech applications due to its high performance in lightweight structures. This trend is clearly appreciated in the aerospace industry, where a big number of parts previouly manufactured with metal have been progressively replace by PMCs. For instance, recently the Boeing 787 have implemented more than 50% by weight of PMCs in the fuselage, enhancing considerably the flight efficiency of this aircraft [1].

However, the increase in the use of this type of material has been slowed because of its poor fatigue behavior. As a consequence, the existence of small cracks might reduce severely the lifetime of a structure [2]. This is the main reason, why surface and structural quality demands are extremely high for composite parts. Therefore, the study optimal machining configurations to reduce cost as well as to avoid massive part rejections is essential in the manufacture of this kind of components.

Unfortunately, the presence of high abrasive fibres or the low thermal resin conductivity convert PMCs in materials difficult to machine. Previous mentioned factors usually occasion a rapid tool wear bending excessively fibres and facilitating the nucleation of internal cracks. Additionally, the incorrect election of cutting parameters (i.e, cutting speed, feed rate, rake angle, etc) cause the appereance of several damage modes as matrix cracking, fibre pullout or delamination [3, 4, 5]. Hence, thousands of trials are neccessary to investigate the effect that all possible cutting configurations have on the post-machining underlying laminate damage.

Factors such as, the high cost of PMCs or cutting tools and operator's time make the experimental trials a non attractive option to address this matter; this option is quite expensive and insert important delays in the industrial production. In contrast, finite element approaches can remarkably reduce the cost and time required in this experimental trials, offering a great cost-

* Corresponding author. Tel.: +44-793-881-2394.
E-mail addresses: fmcepero1@sheffield.ac.uk (F. Cepero-Mejias)., author@institute.xxx (V.A. Phadnis).

2212-8271
10.1016/j.procir.2019.09.005

effective solution to investigate the effect of cutting parameters have on the machining response . One of the most important machining responses to investigate is the chip release mechanisms to achieve a good understanding of the underlying post-machining damage; various 2D micro-mechanical FE models have analysed in detail this matter.

Calzada et al. [6] studied the different fibre failure mechanisms existent for different fibre orientations of 0°, 45°, 90° and 135°. Bending moment from the tool-workpiece interaction was found to be determinant tu cut fibres for fibre orientations of 0° and 135°, while the impact of the tool with the workpiece cause the crush of the fibre for fibre orientations 45° and 90°. Rao et al. [7] assessed various insights about the chip formation for fibre orientations between 15° and 90°. It was concluded that chip release was produced in the matrix between fibre reducing the chip length progressively from 15° to 90° laminates. Finally, Abena et al. [8] developed a 3D micro mechanical model using a novel approach to model the matrix-fibre interface damage. This approach reduced considerably the computational time and increase the accuracy of the results obtained with conventional modelling techniques to model interface damage of cohesive elements and cohesive interactions.

Nevertheless, these micro-mechanical models have a complex pre-processing cost as well as it requires large times to be simulated. These factors make this kind of numerical anlalysis non attractive for the industry, which are more interested in less complicated and quicker analysis capable of predicting accurate results to optimize their production lines. All these capabilities are encompassed in macro mechanical FE models, but to this author's knowledge the chip formation mechanism have been barely investigated in this kind of analysis.

This work offers a novel macro mechanical FE analysis to investigate the chip formation mechanism in machining of composites. The case of UD-CFRP laminates is employed to demonstrate the high capabilities offered for the 2D performed FE model. A novel numerical algorithm in composite machining which accounts first the damage propagation and subsequently the chip fracture is successfully implemented. Well-known composite failure criteria of Hashin and Puck are considered to determine fibre and matrix damage initiation modes, respectively. Later, a linear energy-based degradation of mechanical properties is applied selectively in different components of the stiffness matrix. Finally, shear, matrix crushing and fibre-matrix debonding failures are accounted in this model to produce the chip fracture; this is accomplished eroding element following various strain-based considerations. Numerical predictions are validated using the experimental machining forces extracted by Iliescu et al.[9] in his trials.

Nomenclature

FE	Finite element
PMC	Polymer matrix composite
CFRP	Carbon fibre reinforced polymer
σ_{ij}	Stress vector values in directions "i" and "j""
E_{11}, E_{22}	Young modulus in fibre and transverse directions
G_{12},ν_{12}	Shear laminate modulus and poisson coefficient
X_T, X_C	Fibre tensile and compressive strength
Y_T, Y_C	Matrix tensile and compressive strength
S	Shear laminate strength
$p_{\perp\parallel}^{(+)}$	Slope of the fracture envelope (normal stress - longitudinal/transverse shear stress) curve in traction states when normal stress is 0
$R_{\perp}^{(+)A}$	Fracture resistance of the fracture plane due to transverse stresses
$R_{\perp\parallel}^{A}$	Fracture resistance of the fracture plane due longitudinal/transverse shear stresses
$R_{\perp\perp}^{A}$	Fracture resistance of the fracture plane due to transverse/transverse shear stresses
$\delta_{I,eq}$	Equivalent displacement associated to a damage mode
$\delta_{I,eq}^{0}$	Equivalent displacement associated to a damage mode when it is 0
$\sigma_{I,eq}^{0}$	Equivalent stress associated to a damage mode when it is 0
$\delta_{I,eq}^{f}$	Equivalent displacement associated to a damage mode when it is 1
G_I^C	Critical fracture toughness associated to a damage mode

2. FE model characterization

In this work, an explicit numerical analysis is developed using the numerical software package of Abaqus/CAE. For model validation sake, same cutting conditions employed in Iliescu et al. [9], for the orthogonal cutting of UD-CFRP laminates, have been modelled. Cutting tool geometry analysed is showcased in Table -, while mechanical properties and strength of the CFRP simulated are show in Tables -, respectively.

Table 1. Cutting parameters simulated.

Cutting variables	Simulated machining configuration
Rake angle (α)	0°
Relief angle (β)	7°
Tool edge radius (μm)	10
Depth of cut (mm)	0.2
Cutting speed (mm/s)	100
Fibre orientations	45°

Table 2. CFRP composite mechanical properties.

Material	$E_{11}(GPa)$	$E_{22}(GPa)$	$G_{12}(GPa)$	υ_{12}
CFRP [10]	136.6	9.6	5.2	0.29

Table 3. CFRP composite strength properties.

Material	$X_T(MPa)$	$X_C(MPa)$	$Y_T(MPa)$	$Y_C(MPa)$	$S(MPa)$
CFRP [10]	1500	900	27	200	80

2.1. Mesh, geometry and contact model definition

Workpiece dimensions simulated are 2 mm width per 1 mm height to obtain a good numerical accuracy without a high computational cost. Quadrilateral structured meshed elements CPSR4 are employed with a minimum element size of 5 μm at the cutting region and 0.1 at the bottom corners, see Fig 1. Cutting tool is modelled as a rigid body to reduce the computational time. This assumption is generally accepted in the modelling of composite machining due to cutter razors experience a negligible deformation during the machining process because of their high rigidity.

Allocation of tool edge radius is in the middle of the simulated CFRP workpiece to emulate the real cutting conditions of a machining process. As a boundary conditions in this model, displacements are totally fixed at the bottom and the horizontal movement is restricted in the lateral side of the laminate. Tool-workpiece contact is modelled using the option surface-node surface contact available at Abaqus/Explicit. A constant Coulomb friction coefficient of 0.5 is applied in this work, similarly as it is conducted in other publications related to this field [10, 11].

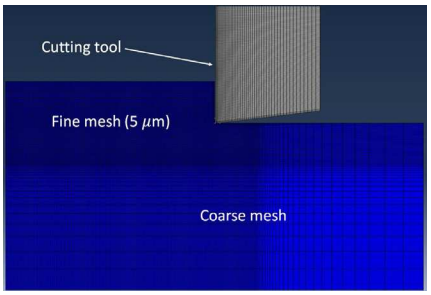

Fig. 1. Mesh distribution of cutting and CFRP workpiece simulated.

3. Composite damage algorithm

An user-defined fortran subroutine VUMAT is developed to introduce the composite damage algorithm employed in this work. This damage algorithm contain two separate phases: (1) damage propagation and (2) chip fracture. In the first phase, the crack path is detected reducing progressively the mechanical properties of the affected meshed elements, while in the second phase the chip is created eroding the previously damaged elements. More detailed information about these statements is found in the following lines.

3.1. Damage propagation

To predict the composite damage propagation along the machining process, four different damage modes are accounted in this model: fibre traction (d_{ft}), fibre compression (d_{fc}), matrix traction (d_{mt}) and matrix compression (d_{mc}). It is implemented using a similar technique employed by Cepero-Mejias et al. [12], distributing the damage coefficients in the stiffness matrix as shown in Eq. 1.

$$\frac{1}{D}\begin{bmatrix} (1-d_f)E_{11} & (1-d_f)(1-d_m)\nu_{21}E_{11} & 0 \\ (1-d_f)(1-d_m)\nu_{12}E_{22} & (1-d_m)E_{22} & 0 \\ 0 & 0 & (1-d_s)G_{12} \end{bmatrix} \quad (1)$$

$$where\ D = 1-(1-d_f)(1-d_m)\nu_{12}\nu_{21} \quad ; \quad d_s = 1-(1-d_{ft})(1-d_{fc})(1-d_{mt})(1-d_{mc})$$
$$d_f = max\{d_{ft}, d_{fc}\}\ ;\ d_m = max\{d_{mt}, d_{mc}\}\ ;\ d_I \in [0,1]\ and\ I = (ft, fc, mt, mc)$$

Fibre and matrix damage initiation is predicted using the well-known Hashin and Puck failure criteria, respectively. In the case of the fibre, Hashin accounts different failures in traction or compression tensional states. For traction, both shear and longitudinal are considered to start the failure, while in compression only longitudinal stresses are relevant, as shown in Eqs. 2 and 3.

- Fibre traction ($\sigma_{11} \geq 0$)

$$\left(\frac{\sigma_{11}}{X_T}\right) + \left(\frac{\sigma_{12}}{S}\right) \geq 1 \quad (2)$$

- Fibre compression ($\sigma_{11} < 0$)

$$\left|\frac{\sigma_{11}}{X_C}\right| \geq 1 \quad (3)$$

For predicting the matrix failure, Puck proposed three separate failure modes Mode A, Mode B and Mode C, which are described below and illustrated in Eqs. 4, 5 and 6.

- Mode A: Matrix damage associated to positive transversal stresses.
- Mode B: Matix damage mode attributed to compression transversal stresses with a high shear contribution.
- Mode C: Matix damage mode related to high compression transversal stresses with a low shear contribution.

- Matrix Mode A ($\sigma_{22} \geq 0$)

$$\sqrt{\left(\frac{\sigma_{12}}{R^A_{\perp\parallel}}\right)^2 + \left(1-\frac{p^{(+)}_{\perp\parallel}}{R^A_{\perp\parallel}}R^{(+)A}_{\perp}\right)^2\left(\frac{\sigma_{22}}{R^{(+)A}_{\perp}}\right)^2} + \frac{p^{(+)}_{\perp\parallel}}{R^A_{\perp\parallel}}\sigma_{22} \geq 1 \quad (4)$$

- Matrix Mode B ($\sigma_{22} < 0\ and\ \sigma_{22} > -R^A_{\perp\perp}$)

$$\sqrt{\left(\frac{\sigma_{12}}{R^A_{\perp\parallel}}\right)^2 + \left(\frac{p}{R}\right)^2\sigma_{22}^2} + \left(\frac{p}{R}\right)\sigma_{22} \geq 1 \quad (5)$$

- Matrix Mode C ($\sigma_{22} \leq -R^A_{\perp\perp}$)

$$\frac{1}{2\left[1+\left(\frac{p}{R}\right)R^A_{\perp\perp}\right]}\left[\left(\frac{\sigma_{12}}{R^A_{\perp\parallel}}\right)^2 + \left(\frac{\sigma_{22}}{R^A_{\perp\perp}}\right)^2\right]\frac{R^A_{\perp\perp}}{-\sigma_{22}} \geq 1 \quad (6)$$

In this work, because only one matrix damage mode in compression states is studied (d_{mc}), this damage is activated after either Mode B or Mode C failure conditions is reached. More detailed information about Puck's failure criteria is found in [13]. After damage initiation occurs, a mechanical linear softening

is performed. This softening is based on the principles of the continuum damage mechanics (CDM) theory, which gradually reduces the material mechanical properties until achieving the total or partial degradation. In this particular case, the degradation is applied to achieve the fracture energy for every damage mode studied (G_{IC}) through Eq. 7- initial and final equivalent displacements are calculated as expressed in Eqs. 8 and 9, respectively.

$$d_I = \frac{\delta^f_{I,eq}\left(\delta_{I,eq} - \delta^0_{I,eq}\right)}{\delta_{I,eq}\left(\delta^f_{I,eq} - \delta^0_{I,eq}\right)} \tag{7}$$

$$\delta^0_{I,eq} = \frac{\delta_{I,eq}}{F_I} \tag{8}$$

$$\delta^f_{I,eq} = \frac{2G^c_I F_I}{\sigma_{I,eq}} \tag{9}$$

Finally, a maximum damage component of 0.99 for fibre and matrix damage modes is considered in this work to avoid the common element distortion that take place in this kind of models [14].

3.2. Chip fracture

The process of chip formation have been barely studied because of the intrinsic difficulty of addressing this matter in macro mechanical FE models. In this document, four types of failures are accounted shear, fibre/matrix debonding, matrix crushing and fibre buckling. The fracture is induced after a big amount of deformation is produced enough for allowing the total fibre or matrix damage degradation and for avoiding element distortion problems. The strains utilised in this work are collected in the following bullet points.

- Shear failure $\Rightarrow |\varepsilon_{12}| \geq 0.4$
- Fibre/matrix debonding $\Rightarrow \varepsilon_{22} \geq 0.2$
- Matrix crushing failure $\Rightarrow \varepsilon_{22} \leq -0.6$
- Fibre buckling $\Rightarrow \varepsilon_{11} \leq -0.1$

4. Model validation and ongoing work

For the sake of validation, the numerical cutting forces obtained for laminates with a fibre orientation of 45° are compared with the forces extracted from Iliescu et al. [9] trials. Average numerical forces have been calculated in the region where elements are deleted to produce the chip fracture, as shown in Fig. 2. Numerical and experimental average forces differs in a 5.5% which represents a strong correlation for this kind of analysis and add credibility to the proposed FE model predictions.

However, this FE model contain limitations that should be improved in the future. For instance, the prediction of the thrust force is considerably low in comparison with experimental findings, as shown in Fig 3. This issue mainly occurs because of the spring back phenomenon [12, 14]- partial thickness recovery after tool pass away - is not address in this work. Fortunately, this

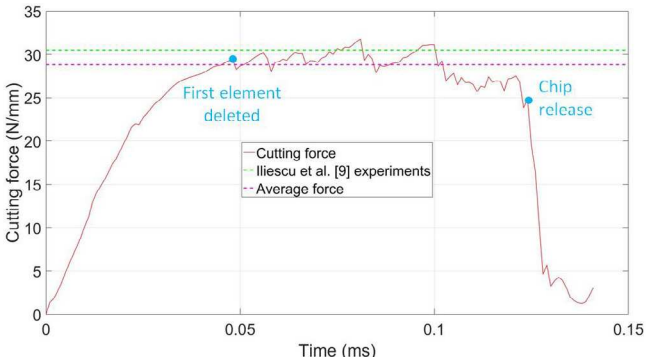

Fig. 2. Cutting force validation of the of the orthogonal cutting with a fibre orientation of 45°.

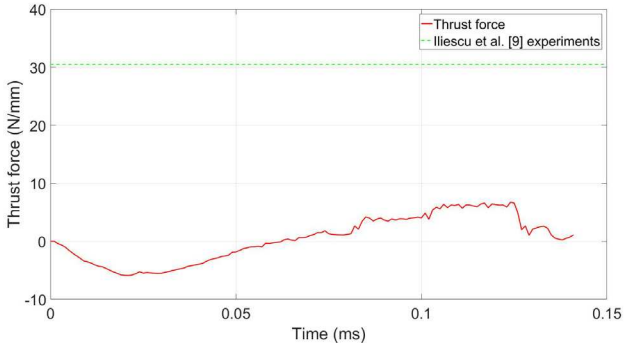

Fig. 3. Experimental and numerical thrust forces of the orthogonal cutting with a fibre orientation of 45°.

phenomenon is not key to predict the chip formation which is the factor studied in this publication.

In the case of machining composite laminates with a fibre orientation of 45° chip is formed along the matrix parallel to the fibres, as it investigated by Arola et al. [15]. Hence, as the simulated chip has an angle closed to 45°, as illustrated in Fig 4, it could be concluded that the chip mechanism have been predicted with high accuracy. Finally, in this kind of fracture, the predominant failure observed is the shear failure detecting high shear deformations in the region around the crack is propagated.

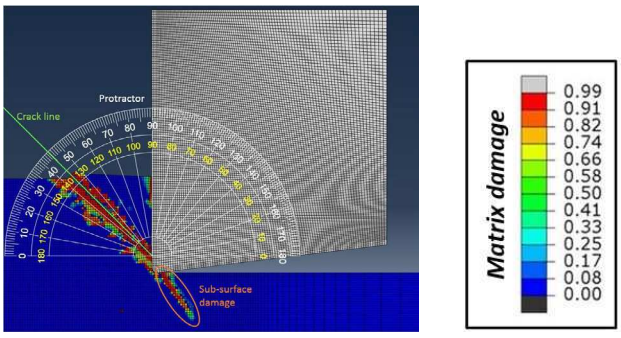

Fig. 4. Chip fracture representation at the end of the simulation time.

Other fibre orientations in the range between 0-180° will be analysed using this methodology in more detail in the future. For a fibre orientation of 0°, fibre micro-buckling is assessed for rake angles equal or inferior to 0°; for positive rake angles

the model predicts the initial matrix delamination and the posterior shear failure of the fibre to release this particular chip. Shear and fibre/matrix debonding failure is observed for positive fibre orientations (15-75°). In the case of 90° laminates, an internal vertical crack is created because of the fibre/matrix debonding created because of the tool push away the fibres. Finally, in negative fibre orientations a shear fibre fracture perpendicular to fibre direction is observed with an internal crack propagation parallel to the fibre orientation.

In addition, after the implementation of various numerical components in the constitutive equations, the modelling of 3D FE models has been possible, see Fig 5. Similar chip formation mechanisms and subsurface damage investigated in 2D models have been obtained. For instance, this matter is observed with the illustration of the chip fracture of 45° 3D laminates in Fig 6. Finally, this numerical methodology offer a potent tool to model other more complex machining operations such us oblique cutting, drilling or edge trimming; further investigations in this directions will be conducted in the future.

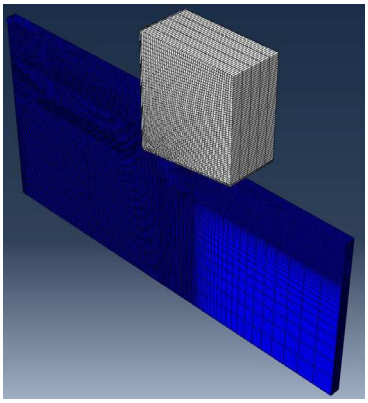

Fig. 5. Numerical 3D FE model representation.

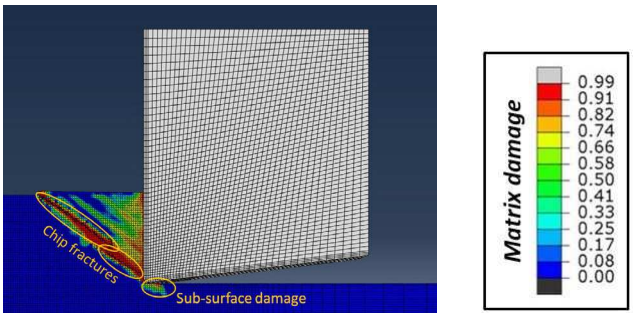

Fig. 6. Chip fracture representation at the end of the simulation time in 3D FE models.

5. Conclusions

This work propose a novel numerical approach to study the chip formation mechanism in the machining of PMCs. Effectiveness of the damage algorithm employed have been corroborated with the validation of the FE model using the cutting forces extracted from Iliescu et al. [9]. Hashin and Puck's failure criteria have been used to determine damage in fibre and matrix respectively. Damage propagation to track the oncoming fracture crack pathway have been applied with an energy-based linear softening. Finally, an element erosion algorithm have been successfully implemented to model four different composite fracture modes: (1) shear failure, (2) fibre/matrix debonding, (3) matrix crushing and (4) fibre micro-buckling.

In this article, just the case of a laminate with a fibre orientation of 45° is assessed. Thus, a wide range of laminates with fibre orientations between 0-180 ° needs to be still investigated.In addition, other more complex machining operations such as edge trimming, oblique cutting or drilling could be modelled using the same methodology exposed in this document. Hence, the use of this FE model to predict the chip and damage during the machining process will be extended to develop interesting insights in the machining of PMCs in a short future.

Acknowledgements

This work was funded by the Engineering and Physical Sciences Research Council (EPSRC) institution with the grant EP/L016257/1 and a special mention is deserved to the Industrial Doctoral Centre (IDC) of Sheffield for their effective technical support in the development of this project.

References

[1] Boeing, "Boeing 787 Dreamliner," 2018.
[2] O. Nixon-Pearson and S. Hallett, "An experimental investigation into quasi-static and fatigue damage development in bolted-hole specimens," *Composites Part B: Engineering*, vol. 77, pp. 462 – 473, 2015.
[3] N. A. Abdullah, J. L. Curiel-Sosa, Z. A. Taylor, B. Tafazzolimoghaddam, J. L. Martinez Vicente, and C. Zhang, "Transversal crack and delamination of laminates using XFEM," *Composite Structures*, vol. 173, pp. 78–85, 2017.
[4] C. Zhang, J. L. Curiel-sosa, and T. Quoc, "Meso-scale progressive damage modeling and life prediction of 3D braided composites under fatigue tension loading," *Composite Structures*, vol. 201, no. June, pp. 62–71, 2018.
[5] J. L. Curiel-sosa, B. Tafazzolimoghaddam, and C. Zhang, "Modelling fracture and delamination in composite laminates : Energy release rate and interface stress," *Composite Structures*, vol. 189, no. January, pp. 641–647, 2018.
[6] K. A. Calzada, S. G. Kapoor, R. E. Devor, J. Samuel, and A. K. Srivastava, "Modeling and interpretation of fiber orientation-based failure mechanisms in machining of carbon fiber-reinforced polymer composites," *Journal of Manufacturing Processes*, vol. 14, no. 2, pp. 141–149, 2012.
[7] G. Venu Gopala Rao, P. Mahajan, and N. Bhatnagar, "Machining of UD-GFRP composites chip formation mechanism," *Composites Science and Technology*, vol. 67, no. 11-12, pp. 2271–2281, 2007.
[8] A. Abena, S. L. Soo, and K. Essa, "Modelling the orthogonal cutting of UD-CFRP composites: Development of a novel cohesive zone model," *Composite Structures*, vol. 168, pp. 65–83, 2017.
[9] D. Iliescu, D. Gehin, I. Iordanoff, F. Girot, and M. E. Gutiérrez, "A discrete element method for the simulation of CFRP cutting," *Composites Science and Technology*, vol. 70, no. 1, pp. 73–80, 2010.
[10] C. Santiuste, X. Soldani, and M. H. Miguélez, "Machining FEM model of long fiber composites for aeronautical components," *Composite Structures*, vol. 92, no. 3, pp. 691–698, 2010.

[11] X. Soldani, C. Santiuste, A. Muñoz-Sánchez, and M. H. Miguélez, "Influence of tool geometry and numerical parameters when modeling orthogonal cutting of LFRP composites," *Composites Part A: Applied Science and Manufacturing*, vol. 42, no. 9, pp. 1205–1216, 2011.

[12] F. Cepero-Mejías, Z. C. Curiel-Sosa, J.L., and V. Phadnis, "Effect of cutter geometry on machining induced damage in orthogonal cutting of ud polymer composites : Fe study," *Composite Structures*, vol. 214, pp. 439–450.

[13] A. Puck and H. Schurmann, "Failure Analysis of Frp Laminates By Means of Physically Based Phenomenological Models *," *Composites Science and Technology*, vol. 3538, no. 96, pp. 1633–1662, 1998.

[14] L. Lasri, M. Nouari, and M. El Mansori, "Modelling of chip separation in machining unidirectional FRP composites by stiffness degradation concept," *Composites Science and Technology*, vol. 69, no. 5, pp. 684–692, 2009.

[15] D. H. Wang, M. Ramulu, and D. Arola, "Orthognal cutting mechanism of graphite/epoxy composite. Part II: Multi-directional laminate," *Int. J. Mach. Tools Manufact.*, vol. 35, no. 12, pp. 1639–1648, 1995.